Temperature Increase in Human Organs Due to Over-Exposure to Electromagnetic Radiations from Mobile Devices and Base Stations: A Comparison Study

Wessapan T[1,*], and Rattanadecho P[2]

[1] School of Aviation, Eastern Asia University, Pathumthani 12110
[2] Center of Excellence in Electromagnetic Energy Utilization in Engineering (CEEE)
Department of Mechanical Engineering, Faculty of Engineering,
Thammasat University (Rangsit Campus), Pathumthani 12120
*Corresponding Author. E-mail: teerapot@eau.ac.th

Abstract

People are continuously exposed to electromagnetic (EM) sources in their vicinity which has been generated by electronic devices such as those found in mobile phones, portable devices, and base stations. This study aims to investigate the temperature increase in human organs due to EM fields emitted from the mobile base stations and portable devices at over-exposure conditions. This study systematically investigates and models the effects of distance to an EM source and radiated power on heat transfer in each organ e.g. testis, intestine, bladder, etc. The specific absorption rate (SAR) and the temperature increases in the tissue during exposure to EM fields are obtained by numerical simulation of the bioheat transfer equation and the EM wave propagation as described by Maxwell's equations. The findings indicate that the exposure distance from the EM source significantly influences the electric field, SAR and temperature distribution in each organ. Moreover, the tissue dielectric properties also affect the temperature distribution patterns within the tissue. These findings may enable us to determine the exposure limits for the power output of the wireless transmitter, and its distance from the human. Furthermore, the findings can be used as a guideline to clinical practitioners in EM related the interaction of the radiated waves with the human body.

Keywords: Electromagnetic fields; Temperature increase; Specific absorption rate; Human organ.

1. Introduction

Whether or not electromagnetic (EM) fields induced from a strong EM source potentially pose any direct or indirect health hazards for humans is uncertain. Further, the human body's response to thermo-physiological phenomena is currently not well understood. In recent years, the utilization of electromagnetic (EM) waves in various applications has been increasing rapidly in daily life, including mobile phones, tablet, laptops and microwave cooking. The high intensity electromagnetic fields (EMFs) of different power levels and frequencies penetrate deep into the human body and raise the temperature in the tissues, causing health risks [1, 2]. The concern is heightened when the power absorption in the sensitive area in close proximity to the intense radiation (near-field exposure) source induces a temperature increase inside it. While there has been a substantial growth in the use of mobile communication services over the last few years. With this growth comes the inevitable increase in the number of base station sites, accompanied by public concern for possible impacts of these communication systems (far-field exposure).

However, the difference between near-field and far-field temperature response of the human body EM filed is still not well understood. In order to gain insight into the phenomena in the human body related to the temperature increase induced by near and far fields, a detailed knowledge of the absorbed power distribution as well as the temperature distribution is necessary. Therefore, this study aims to compare between the temperature increase in human organs due to over-exposure to electromagnetic radiations from near-field sources mobile devices and far-field sources such as base stations. Although safety standards in terms of the maximum SAR values are regulated [3], they are not stated in terms of the maximum temperature increase in the tissue caused by EM energy absorption, which is the actual influence of the dominant factors inducing adverse physiological effects. According to it is prohibited to study SAR and heat transfer in a living human to EMFs, therefore numerical

analysis of the heat transfer in human body exposed to EM fields has provided useful information on the absorption of EM energy under a variety of exposure conditions.

Calculating the spatially-induced electric field, SAR and temperature increase becomes more complex when the human body is non-uniform in shape and contains several organs. Most studies of the human body's exposure to EM fields have not considered a realistic domain with complicated organs of several types of tissue. In order to provide information on the levels of exposure and health effects from EM radiation, it is essential to simulate both the EM field and heat transfer within an anatomically based human body model to represent the actual processes of heat transfer within the human organ. This work was substantially extended from earlier works [6] by focusing on the near-field effect and including more tissue layers to complete the knowledge in the subject area.

This study investigates the temperature increase in human organs due to EM fields emitted from the mobile base stations and portable devices at over-exposure conditions. The study compared the EM absorption characteristic between near-field exposure and far-field exposure. In the near-field case, the model is exposed to the 1 W of EM radiation at 10 cm distance. This case represents the exposure level of the human body to the radiation of portable device. In the far-field case, the model is exposed to the 100W of EM radiation at 10 m distance. This case represents the exposure level of the human body to the radiation of mobile phone base station.

A 2D heterogeneoushuman model was used to simulate the SAR and the temperature increases induced by EM energy. The model comprises eleven types of tissue: the skin, fat, muscle, bone, testis, large intestine, small intestine, bladder, blood, stomach and liver. The EM wave propagation was investigated by using Maxwell's equations. An analysis of the heat transfer was investigated using a bioheat transfer model. In this study, the frequency of 900 MHz is chosen for our simulations as the frequency used globally in a wide range of applications including Global System for Mobile Communications (GSM) services. In the simulation work, the model excluded the presence of clothing in order to ease the modeling procedures. In the simulation, the human body has an initial temperature of 37 degree Celsius. The convective heat transfer coefficient of the skin surface is assumed to be 20 $W/m^2.K$.

2. Formulation of the problem

Near-field sources such as mobile phones and portable wireless routers operate in the close vicinity of the body and can cause temporarily high local exposure. While the far-field sources such as mobile phone base station have higher radiated power which lead to a range of different effects. For adequate study of the energy absorbed in human tissue caused by EM near-field and far-field exposures, the contribution of different EM sources to the human exposure of different body tissues is required. Fig. 1 shows human exposure to near-field and far-field EM radiations. Due to ethical considerations, exposures of the human to EM fields for experimental purposes are limited. It is more convenient to develop a realistic human model through numerical simulation. A highlight of this work is the comparison of the temperature increase in a piecewise-homogeneous human model at different exposure conditions (near-field and far-field). The analyses of the electric fields, SAR and heat transfer in the model will be illustrated in Section 3. The system of governing equations as well as the initial and boundary conditions are solved numerically using the finite element method (FEM) via COMSOL™ Multiphysics.

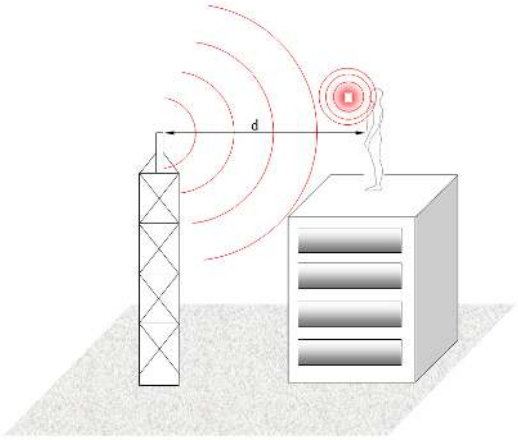

Fig. 1 Human exposure to EM radiations from mobile device and base station

3. Methods and model

3.1 Physical model

Fig. 2 shows the physical domain of this study, in which interactions between the human body and the EM radiation from antenna take place. The model has a dimension of 400 mm in

width and 525 mm in height and comprises 11 types of tissue which are skin, fat, muscle, bone, testis, large intestine, small intestine, bladder, blood, stomach and liver. These tissues have different dielectric and thermal properties.

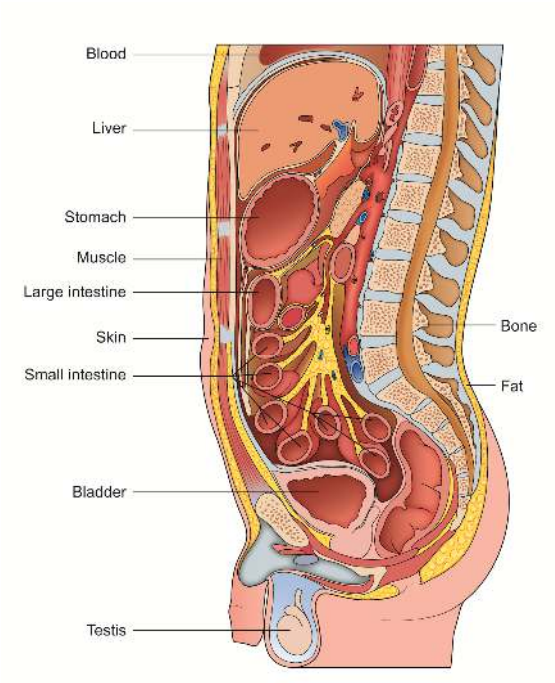

Fig. 2 Human body vertical cross section

The dielectric and thermal properties are obtained according to the comprehensive literature review of Hasgall [4] (www.itis.ethz.ch/database), the dielectric properties of which are largely identical to those proposed by Gabriel et al. [5]. The dielectric and thermal properties of the tissues are given in Tables 1 and 2 , respectively. Each tissue is assumed to be homogeneous and electrically as well as thermally isotropic. There is no effect on the chemical reaction and phase change within the tissue. The antenna's feed point, located at the left side of the body with different positions, is considered as a near-field and far-field radiation sources for the human body. The antenna is excited at the center feed point, and the transmitted power is determined as the complex product of the current and voltage at the feed point. The antennas used operate at 9 0 0 MHz frequency and transmits the radiated power of 1.0 W, the approximate power of general mobile phone and 100W, the approximate power of mobile phone base station.

Table. 1 Dielectric properties of tissues [4, 5]

	900 MHz	
	ε_r	σ **(S/m)**
Skin	41.4	0.867
Fat	11.3	0.109
Muscle	55.0	0.943
Bone	12.5	0.143
Testis	60.6	1.21
Large intestine	57.9	1.08
Small intestine	59.5	2.17
Bladder	18.9	0.383
Blood	61.4	1.54
Stomach	65.1	1.19
Liver	46.8	0.855

Table. 2 Thermal properties of tissues [4]

Tissue	ρ **(Kg/m^3)**	k **(W/m°C)**	C **(J/kg°C)**	Q_{met} **(W/m^3)**	ω_b **(1/s)**
Skin	1109	0.37	3391	1829	0.001855
Fat	911	0.21	2348	464.6	0.0005775
Muscle	1090	0.49	3421	991.9	0.0006475
Bone (cortinal)	1908	0.32	1313	286.2	0.000175
Testis	1082	0.52	3778	3343.38	0.0035
Large intestine	1088	0.54	3655	12892.8	0.0133875
Small intestine	1030	0.49	3595	16366.7	0.017955
Bladder	1086	0.52	3581	1314.06	0.001365
Blood	1050	0.52	3617	-	-
Stomach	1088	0.53	3690	7757.44	0.00805
Liver	1079	0.52	3540	10714	0.01505

3.2 Equations for EM wave propagation analysis

The mathematical models are developed to predict the electric fields and the SAR with respect to the temperature gradient in the model. To simplify the problem, the following assumptions are made:

1. The EM wave propagation is modeled in two dimensions.
2. The EM wave interaction with the tissue proceeds in the open region.
3. The free space is truncated by a scattering boundary condition.
4. The model assumes that the dielectric properties of each tissue are constant.
5. The radiated waves from the dipole are characterized by transverse electric (TE) fields.

The EM wave propagation is calculated using Maxwell's equations [6], which mathematically describe the interdependence of the EM waves. The general form of Maxwell's equations is simplified to demonstrate the EM field that penetrates into the tissue as follows:

$$\nabla\times\left(\frac{1}{\mu_r}\nabla\times E\right)-k_0{}^2\left(\varepsilon_r-\frac{j\sigma}{\omega\varepsilon_0}\right)E=0 \qquad (1)$$

$$\varepsilon_r=n^2 \qquad (2)$$

where E is the electric field intensity (V/m), μ_r is the relative magnetic permeability, n is the refractive index, ε_r is the relative dielectric constant, $\varepsilon_0=8.8542\times10^{-12}$ F/m is the permittivity of free space, σ is the electric conductivity (S/m), $j=\sqrt{-1}$ and k_0 is the free space wave number (m^{-1}).

3.2.1 Boundary condition for wave propagation analysis

The boundary conditions along the interfaces between different mediums, namely, between air and tissue, are considered as a continuity boundary condition:

$$n\times(H_1-H_2)=0 \qquad (3)$$

The outer sides of the calculated domain, i.e., free space, are considered as a scattering boundary condition to eliminate reflections:

$$n\times\left(\nabla\times E\right)-jkE=0 \qquad (4)$$

where k is the wave number (m^{-1}), n is the normal vector, $j=\sqrt{-1}$, and H is the magnetic field (A/m).

3.3 Interaction of EM fields and human tissues

To quantify the exposure conditions and the resulting responses for the various biological tissues, the specific absorption rate (SAR) is used. The exposure limits used by the International Commission of Non-Ionizing Radiation Protection (ICNIRP) are expressed in terms of SAR [3]. The SAR is defined as the power dissipation rate normalized by the material density. The SAR is given by

$$SAR=\frac{\sigma}{\rho}|E|^2 \qquad (5)$$

where E is the electric field intensity (V/m), σ is the electric conductivity (S/m) , and ρ is the tissue density (kg/m^3).

3.4 Equations for heat transfer analysis

To solve the thermal problem, the coupled effects of the EM wave propagation and the unsteady bioheat transfer are investigated. To reduce the complexity of the problem, the following assumptions are made:
1. The tissue is a bio-material with constant thermal properties.
2. There is no phase change of substance in the tissue.
3. There is no chemical reaction in the tissue.
4. The heat transfer is modeled in two dimensions.
5. The thermal properties of the tissues are constant.

The temperature increase within the human body is obtained by solving Pennes' bio-heat equation [7]. The transient bioheat equation describes effectively how heat transfer occurs within the tissue, and the equation can be written as

$$\rho C\frac{\partial T}{\partial t}=\nabla\cdot\left(k\nabla T\right)+\rho_b C_b\omega_b\left(T_b-T\right)+Q_{met}+Q_{ext} \qquad (6)$$

where ρ is the tissue density (kg/m^3), C is the heat capacity of tissue (J/kg K), k is the thermal conductivity of tissue (W/m K), T is the tissue temperature (°C), T_b is the temperature of blood (°C), ρ_b is the density of blood (kg/m^3), C_b is the heat capacity of blood (J/kg K), ω_b is the blood perfusion rate (1/s), Q_{met} is the metabolism heat source (W/ m^3) and Q_{ext} is the external heat source (electromagnetic heat-source density) (W/ m^3).

In the analysis, heat conduction between the tissue and blood flow is approximated by the blood perfusion term, $\rho_b C_b\omega_b\left(T_b-T\right)$.

The external heat source term is equal to the resistive heat generated by the electromagnetic field (electromagnetic power absorbed), which is defined as

$$Q_{ext} = \frac{1}{2}\sigma_{tissue}\left|\overline{E}\right|^2 = \frac{\rho}{2}\cdot SAR \qquad (7)$$

3.4.1 Boundary condition for heat transfer analysis

Heat transfer is considered only in the human model, which does not include parts of the surrounding space. As shown in Fig. 3, the outer surface of the human model is considered to be a convective boundary condition:

$$n.(k\nabla T) = h(T_{\inf} - T) \qquad (8)$$

It is assumed that no contact resistance occurs between the layers of the human tissue. Therefore, the internal boundaries are assumed to be continuous:

$$n\cdot(k_u\nabla T_u - k_d\nabla T_d) = 0 \qquad (9)$$

$$T_u = T_d \qquad (10)$$

3.5 Calculation procedure

In this study, the finite element formulations of the coupled electromagnetic–bioheat transfer model in the human body are carried out over the entire domain. In order to obtain a good approximation, a fine mesh is specified in the sensitive areas. This study provides a variable mesh method for solving the problem, as shown in Fig. 3 . The system of governing equations as well as the initial and boundary conditions are then solved. All computational processes are implemented using COMSOL™ Multiphysics, to demonstrate the phenomenon that occurs in the organs exposed to the EM fields.

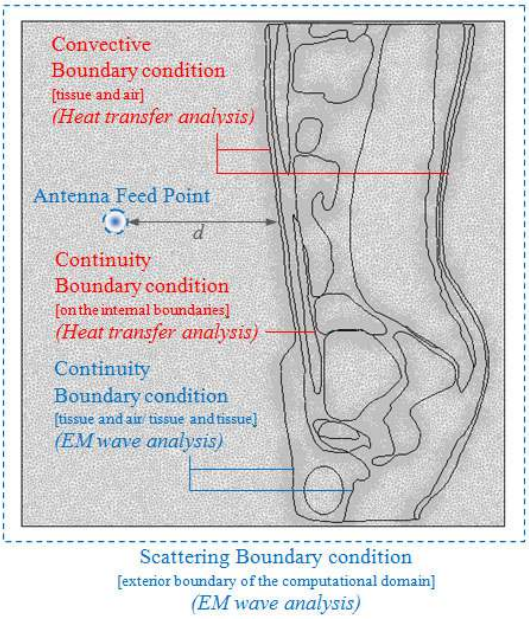

Fig. 3 A finite element mesh of computational model and boundary condition for analysis of EM wave propagation and heat transfer

The 2 D model is discretized using triangular elements and the Lagrange quadratic elements are then used to approximate the temperature and SAR variations across each element. A grid independence test is carried out to identify the appropriate number of elements required. This grid independence test leads to a mesh with approximately 100,000 elements. It is reasonable to assume that, at this element number, the accuracy of the simulation results is independent of the number of elements.

4. Results and discussion

In the model, the electric field, SAR and temperature increase distributions of the near-field and far-field are systematically investigated. The model is exposed to the dipole source at the frequency of 900MHz to illustrate the penetrated EM field and its temperature response inside the body. In the near-field case, the model is exposed to the 1 W EM radiation at 10 cm distance. In the far-field case, the model is exposed to the 100W EM radiation at 10 m distance. The numerical analysis of coupled electromagnetic propagation and heat transfer is done by solving the Maxwell and bioheat equations. The dielectric and thermal properties are taken directly from Tables 1 and 2 respectively. The exposed radiated power used in this study refers to the International Commission of Non-Ionizing Radiation Protection (ICNIRP) standard for safety levels at the maximum SAR value of 2 W/kg (general public exposure) and 10 W/kg (occupational exposure) [3].

4.1 Verification of the model

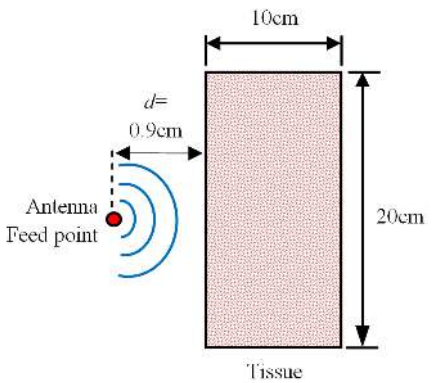

(a)

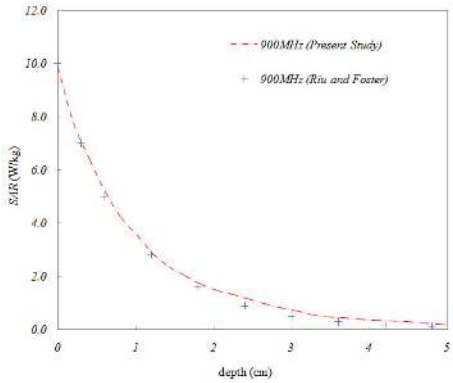

(b)

Fig. 4 Validation of the mathematical model:

(a) The computational domain for validation

(b) Comparison of the calculated SAR values to the SAR values obtained by Riu and Foster [8]

Before we can solve the problem, an initial numerical validation is required to support the results stated in this paper. In order to verify the accuracy of the present numerical models, the simple case of the simulated results is validated against the numerical results obtained with the same geometric model obtained by Riu and Foster [8] . The SAR is determined in a homogeneous tissue model from near-field exposure to a dipole antenna. In the validation case, the dipole used operates at 9 0 0 MHz frequency and transmits the radiated power of 0.6 W.

The computational domain and the result of the validation test case is illustrated in Fig. 4 . From the figure, the SAR decreases exponentially in the direction of wave propagation. The obtained result clearly shows good agreement of the SAR value of the tissue between the present solution and that of Riu. This favorable comparison lends confidence in the accuracy of the present numerical model and ensures that the numerical model can accurately represent the phenomena occurring at the interaction of the EM fields with the tissue.

4.2 Electric field distribution

Fig. 5 shows the simulation of an electric field pattern inside the model exposed to the EM fields in TE mode operating at the frequency of 900 MHz and propagating over the vertical cross-section of the human model. Due to the different dielectric characteristics of the various tissue layers, a different fraction of the supplied EM energy will become absorbed in each layer in the model. Consequently, the reflection and transmission components at each layer contribute to the resonance of the standing wave in the tissue. It can be seen that the highest values of electric fields occur in the outer area of the body, especially in the skin layer. By comparison, the maximum electric field intensity in the outer parts of the body in the case of near-field exposure displays a little bit higher value than that of far-field exposure case. The maximum electric field intensities are 98.905 and 97.597 V/m for the near-field and far-field exposure, respectively. For both cases, the electric fields deep inside the body are extinguished as the electric fields attenuate due to the absorbed EM energy and are then converted to heat. As shown in the figure, the penetration depth of the EM field inside the dispersive lossy tissue decreases as the frequency increases. The EM absorption pattern in the near-field exposure case typically differs significantly from that occurred at far-field exposure case. In the tissue closed to the dipole antenna in the near-field case (Fig.5a), the electric field pattern distributes in the near-circle shape. While for a large distances exposure in the far-field case (Fig.5b), the electric field distribution pattern being similar to the plane wave exposure.

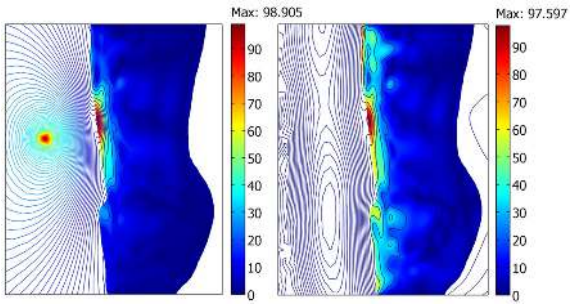

(a) (b)

Fig. 5 Electric field distribution (V/m) in the human model during exposure to the dipole antenna:

(a) 1W at 0.1m distance (near-field)

(b) 100W at 10m distance (far-field)

4.3 SAR distribution

Fig. 6 shows the SAR distribution evaluated on the vertical cross-section of the human model exposed to the EM frequency of 900 MHz. It is evident from the figures that the results of the SAR distribution in the human body (Fig. 6) which are increased corresponding to the electric field distribution (Fig. 5). Besides the electric field intensity, the magnitude of electric conductivity (S/m), and ρ is the tissue density (kg/m^3) in Table 1 and 2 will directly affect the amount of SAR within the human body. This is because the SAR is a function of the electrical conductivity, which corresponds to Eq. (5).

For both cases, the highest SAR values are obtained in the skin surface. The maximum SAR values for the near-field and far-field are 3.824 and 3.723 W/kg respectively. Compared to the ICNIRP standard for the safety level at the maximum SAR value of 2 W/kg (general public exposure) [3], the resulting SAR values at both near-field and far-field are higher than the ICNIRP exposure limits for general public exposure and lower than 10W/kg for occupational exposure limit.

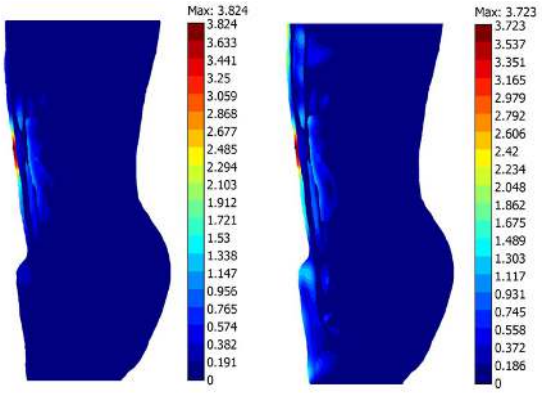

(a) (b)

Fig. 6 SAR distribution (W/kg) in the human model during exposure to the dipole antenna:

(a) 1W at 0.1m distance (near-field)

(b) 100W at 10m distance (far-field)

4.4 Temperature distribution

Since this study has focused on the electromagnetic heating effect in the heterogeneous human model, the effects of an ambient temperature variation have been neglected in order to gain insight into the interaction between the EM fields and the tissue, as well as the correlation between the SAR and the heat transfer mechanism. Therefore, at the skin surface of the human model, the convective boundary condition is applied. The effect of thermoregulation mechanisms has also been neglected due to the small temperature increase that occurs during the exposure process.

In order to study the heat transfer in the tissue, the coupled effects of EM wave propagation and unsteady heat transfer as well as the initial and boundary conditions are then investigated. Due to these coupled effects, the electric field distribution in Fig. 5 and the SAR distribution in Fig. 6 are then transformed into an incremental amount of heat by EMF absorption of the tissue. Fig. 7 shows the steady state temperature increase in the vertical cross-section human model exposed to the near-field (Fig. 7a) and far-field (Fig. 7b) EMFs.

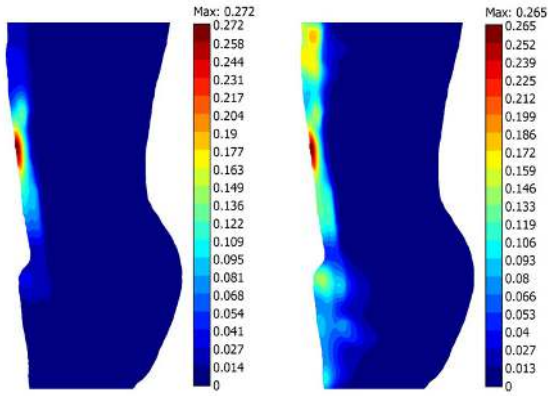

(a) (b)

Fig. 7 Temperature increase distribution (° C) in the human model during exposure to the dipole antenna:

(a) 1W at 0.1m distance (near-field)

(b) 100W at 10m distance (far-field)

For the model exposed to the EMF for 60 minutes, the tissue temperature (Fig. 7) is increased corresponding to the SAR (Fig. 6). This is because the electric fields in the tissue attenuate owing to the energy absorbed and thereafter the absorbed energy is converted to thermal energy, which increases the body temperature. At steady state, the maximum temperature increases are 0.272 °C and 0.265 °C

for the near-field and far-field exposure, respectively. It is found that when the model is subjected to the EM fields at different exposure conditions, the distribution patterns of the temperature are quite different. This is because the difference in the temperature distribution pattern between the two cases is caused by dielectric properties of the tissue, as well as thermal properties of the tissue, which become the dominant mechanisms for the heat transfer.

Fig. 8 Comparison of the temperature increase (°C) in each tissue type for the radiated power of 1W at 0.1m distance (near-field) and 100W at 10m distance (far-field). For both cases, the three highest temperature increases are shown for the skin, fat and muscle.

From the figure, the temperature increases of the skin and fat of the near-field case are higher than that of the far-field. While in the other organs, the far-field case shows the higher values of the temperature increase than that of the near-field. This is because the penetration area of the far-field case is larger than that of near-field case.

In this study, it is found that the temperature increase distributions in the testis are not directly proportional to the local SAR distributions. Nevertheless, these are also related to parameters such as the surrounding tissue temperature, thermal conductivity, dielectric properties, blood perfusion rate, etc.

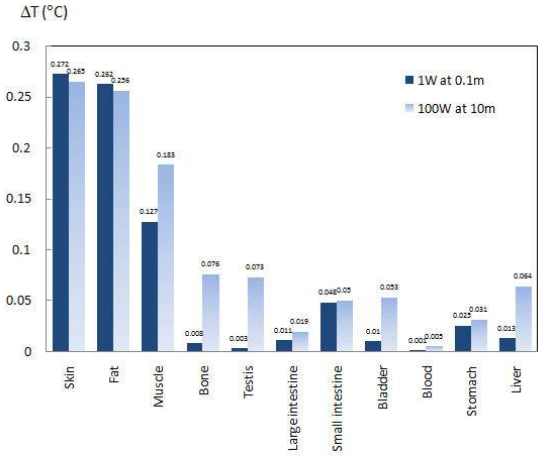

Fig. 8 Comparison of the temperature increase (°C) in each tissue type for the radiated power of 1W at 0.1m distance (near-field) and 100W at 10m distance (far-field).

5. Conclusions

The numerical simulations of the electric field, SAR and temperature distributions in this study show several important features of the energy absorption and temperature increase in the heterogeneous human model during exposure to near-field and far-field EMFs at 900 MHz.

The numerical simulations in this study show several important features of the energy absorption in the human tissue. The electric field distributions display a wavy behavior and show a strong dependence on the exposure distance and the dielectric properties of the tissue. The distribution patterns of the SAR vary corresponding to the electric field intensities. Besides the electric field intensity, the magnitude of the dielectric and thermal properties in each tissue type will directly affect the SAR distribution patterns.

We refer to the SAR safety limit indicated in the Guidelines as 2 W/kg for general public exposure and 10 W/kg for occupational exposure according to ICNIRP. The calculated testis temperature increases are lower than the thresholds for the induction of infertility of 1 °C in both cases. However, in both cases, the SAR values are higher than the general public exposure limits of 2 W/kg but lower than the occupational exposure limit of 10 W/kg specified in the ICNIRP [3].

The results obtained may be of assistance in determining exposure limits for the power output of wireless transmitters, mobile phone and base station for use with humans. In future works, the effect of feed point position will be included in the analysis to represent the actual heat transfer process which occurs in a realistic situation and a more realistic 3D model will be developed for the simulations. This will allow a better understanding of the real situation of the interaction between EM fields and the human body.

- The values obtained represent the accurate phenomena to determine the temperature increase in the human body and indicate the limitations that must be considered as the temperature increases due to EM energy absorption from EM field exposure at different exposure distances.

6. Acknowledgments

The authors gratefully acknowledge the Thailand Research Fund (TRF) and Eastern Asia University.

7. References

[1] A. Hirata, S. Matsuyama, T. Shiozawa, Temperature rises in the human eye exposed to EM waves in the frequency range 0.6–6 GHz, IEEE Trans. Electromagn. Compat 42 (4) (2000) 386–393.

[2] O.P. Gandhi, G. Kang, Some present problems and a proposed experimental phantom for SAR compliance testing of cellular telephones at 835 MHz and 1900 MHz, Phys. Med. Biol. 47 (2002) 1501–1518.

[3] International Commission on Non-Ionizing Radiation Protection: ICNIRP (1998). Guidelines for Limiting Exposure to Time-Varying Electric, Magnetic and Electromagnetic Fields (up to 300 GHz), Health Phys. 74 (1998) 494–522.

[4] Hasgall PA, Di Gennaro F, Baumgartner C, Neufeld E, Gosselin MC, Payne D, Klingenböck A, Kuster N. IT'IS Database for thermal and electromagnetic parameters of biological tissues. Version 3.0, September 1st. 2015. www.itis.ethz.ch/database, DOI: 10.13099/VIP21000-03-0.

[5] Gabriel S, Lau R, Gabriel C. The dielectric properties of biological tissues. II: Measurements in the frequency range 10 Hz to 20 GHz. Phys Med Biol. 41 (1996) 2251–2269.

[6] T. Wessapan, S. Srisawatdhisukul, P. Rattanadecho, Numerical analysis of specific absorption rate and heat transfer in the human body exposed to leakage electromagnetic field at 915 MHz and 2450 MHz, ASME J. Heat Transfer 133 (2011) 051101.

[7] H.H. Pennes, Analysis of tissue and arterial blood temperatures in the resting human forearm, J. Appl. Phys. 85 (1998) 5-34.

[8] P.J. Riu, K.R. Foster, Heating of tissue by near-field exposure to a dipole, IEEE Trans. Biomed. Eng. 46 (8) (1999) 911–917.